Airfoil Parameterization using an Improved Class-Shape Transformation and Chebyshev Polynomials

Andrew Heletkanycz
Graduate Research Assistant
The Pennsylvania State University
University Park, PA, USA

James Coder
Associate Professor
The Pennsylvania State University
University Park, PA, USA

Christopher Thurman
Research Aerospace Engineer
NASA Langley Research Center
Hampton, VA, USA

ABSTRACT

A method for the parameterization of an arbitrary airfoil using a transformation and Chebyshev polynomial interpolation is investigated. The airfoil was transformed into a continuous function using the Class Shape Transformation. A square root spacing was used to smooth out the slope discontinuity found at the origin. This mapping reduces oscillations in the polynomial interpolation caused by the slope discontinuity at the origin. Interpolating a range of NACA 4-digit series airfoils showed that these airfoils could be accurately represented with as little as 10 polynomial terms. However, problems arise with the Class Shape Transformation when trying to parameterize non-analytically defined airfoils. The transformation expects the behavior of the leading edge to be perfectly elliptic, and any deviation from this requirement leads to the divergence of the Class Shape Transformation. As a result, parameterizing with polynomials becomes infeasible for some airfoils. To address this, a conformal mapping-based unwrapping method is suggested.

INTRODUCTION

Many mid-fidelity tools used for aerodynamic predictions of rotorcraft heavily rely on blade element momentum-type methods. These methods traditionally use airfoil tables to provide the performance characteristics of the blade at different spanwise locations. Typically, these airfoil tables use Mach number and angle of attack to define performance characteristics of the airfoil, which do not explicitly account for Reynolds number variations. This may be problematic when characterizing airfoil performance or capturing performance losses due to low-Reynolds-number effects, such as laminar separation bubbles. For advanced air mobility vehicles, this is especially important, as their rotors may operate at lower tip speeds and Reynolds numbers when compared to traditional rotorcraft (Ref. 1).

Airfoil tables are usually generated using airfoil panel method codes, computational fluid dynamics (CFD), or data from wind tunnel tests. Fortunately, analysis with airfoil panel method codes is not as computationally expensive as it once was, due to advances in computing. However, when higher-order methods are required, costs can still accumulate. large eddy simulations (LES) and direct numerical simulations (DNS) are computationally expensive and could be unreasonable for simulations at high Reynolds numbers. Wind tunnel tests are also expensive due to manufacturing costs and testing overhead. When incorporating new airfoils into simulations, a new table needs to be created, which requires new analysis to be performed. To avoid these costs, a surrogate model can be developed to predict aerodynamic performance data from a variety of airfoils without requiring additional experimental or computational studies. As an additional benefit, this surrogate model could be used in reverse for airfoil design. To enable the creation of a surrogate model, an appropriate method to parameterize airfoils first needs to be developed.

Existing parameterization methods for airfoils fall under two categories, deformative or constructive. Deformative methods take a base airfoil and then deform that geometry to create a new airfoil. Constructive methods define an airfoil purely based on a set of parameters. Polynomials, partial differential equations, and singular value decomposition have all been previously used to constructively define airfoils (Ref. 2).

This paper analyzes the use of Kulfan's Class Shape Transformation (Ref. 3) and the parameterization of the resulting shape function with Chebyshev polynomial interpolation. A range of NACA 4-digit airfoils were initially used to determine how well this method parameterizes airfoils. The interpolated airfoils were reconstructed with varying amounts of polynomial modes and compared to the base airfoil both geometrically and through performance data obtained from XFOIL (Ref. 4). XFOIL was used to generate pressure distributions, nondimensional coefficients, and trailing edge boundary-layer values. The parameterization of airfoils that are not defined by equations was also investigated.

Presented at the Vertical Flight Society's 81st Annual Forum & Technology Display, Virginia Beach, VA, USA, May 20–22, 2025.

CLASS SHAPE TRANSFORMATION

Standard Definition

Kulfan's Class Shape Transformation (CST) (Ref. 3) transforms an airfoil into a function space that can be more easily represented using parametric definitions. This transformation begins by defining a general class function, $C(x)$, where x are the chord-normalized abscissas,

$$C(x) = x^{N1}(1-x)^{N2}, \tag{1}$$

with which a shape function, $S(x)$, can be used to separately construct the upper and lower surfaces of the airfoil as

$$S(x) = \frac{y - \Delta y_{TE}}{C(x)}. \tag{2}$$

In this expression, y are the chord-normalized ordinates and Δy_{TE} is the normalized trailing-edge thickness. The exponents $N1$ and $N2$ are set to 0.5 and 1.0 respectively for round nose airfoils with sharp trailing edges.

At $x = 0$ and 1, the class function is zero; however, the value of Eq. 2 nominally approaches a well-defined limit. At the leading edge, the value of the shape function directly relates to the airfoil nose radius as,

$$S(0) = \pm\sqrt{2\frac{R_{LE}}{c}}, \tag{3}$$

where R_{LE} is the radius of curvature at the leading edge and c is the chord length. The limit at the trailing edge is found to be

$$S(1) = \tan\beta + \frac{\Delta y_{TE}}{c}, \tag{4}$$

where β is the boattail angle. The boattail angle for the upper or lower surface is the angle that the upper or lower surface forms at the trailing edge with respect to the horizontal.

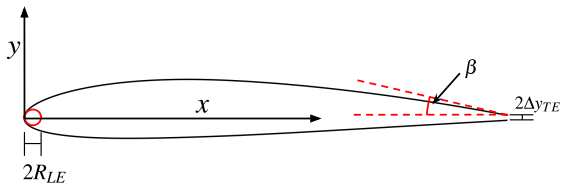

Figure 1: Visualization of CST Parameters.

Unwrapped CST (uCST)

Typical application of the CST results in separate shape functions for the upper and lower surfaces of the airfoil, each defined on $x = [0,1]$. Stanko (Ref. 5) recognized that both the ordinate and abscissa of the lower-surface shape function can be multiplied by -1 to obtain a continuous curve defined on $x = [-1,1]$. This formulation is referred to as unwrapped CST or uCST. The curve need only be continuous, not necessarily smooth, at the origin, since the class of functions will recover a twice-differentiable (or smoother) airfoil definition. Should the uCST shape function be discontinuous at $x = 0$, the resulting airfoil will have a curvature discontinuity at $x = 0$. While some practitioners forgo curvature discontinuity, cf. (Ref. 6) and (Ref. 7), this will lead to unnecessary oscillations in the pressure distribution.

In Kulfan's original work, the shape functions were defined (or deformed) using Bernstein polynomials; however, work by Vassberg et al. (Ref. 8) found that increasing the order of the Bernstein polynomial to add degrees of freedom results in pronounced numerical stiffness that can stall an aerodynamic design optimizer. Alternatively, the use of uCST opens up the possibility of defining the airfoil with orthogonal polynomial bases and improving the matrix conditioning. Stanko (Ref. 5) applied Legendre polynomials to this task, as they are orthogonal with respect to a uniform weighting; however, the extrema of the Legendre polynomials are not consistent in amplitude, which has excessive effect on the airfoil trailing edge. Building on this work, Karman et al. (Ref. 9) used Chebyshev polynomials, which have a consistent amplitude across the entire domain.

Persistent Leading-Edge Pathology

Although uCST is designed to analytically 'unwrap' the airfoil and remove the high curvature at the leading edge, a singular behavior generally persists in the shape functions at $x = 0$. If one considers the general form of an NACA 4-digit series thickness distribution,

$$\eta(x) = a\sqrt{x} + bx + cx^2 + dx^3 + ex^4, \tag{5}$$

the limiting behavior of the shape function is $S(x) = a + b\sqrt{x} +$ higher-order terms as $x \to 0$. Despite the intentions of the CST methodology to remove the high curvature at the leading edge introduced by $\sqrt{x}$ behavior in the thickness distribution, this functional behavior can nevertheless persist in general shape functions. Despite their mathematical simplicity, NACA airfoils are therefore not well represented using rational, finite-degree polynomials in the CST (or uCST) framework. Additionally, using finite-degree polynomials artificially limits the leading-edge shapes that can be represented using CST.

IMPROVED CHEBYSHEV REPRESENTATION

Chebyshev polynomials form two related families, known as the first and second kinds. In this work, Chebyshev polynomials of the first kind were used to interpolate the shape functions, in lieu of Legendre, Bernstein, or Chebyshev polynomials of the second kind, because they have a constant magnitude in the domain of [-1, 1]. For this range, Chebyshev

polynomials are also orthogonal with respect to a weighting of $\frac{1}{\sqrt{1-x}}$.

Chebyshev polynomials of the first kind are defined by

$$T_n(x) = \cos\left(n \arccos\left(x\right)\right), \tag{6}$$

where n is the degree of the desired Chebyshev polynomial. Using these polynomials, a function may be represented as a linear combination,

$$f(x) = \sum_{n=0}^{N} a_n T_n, \tag{7}$$

where a_n are coefficients that are solved using a linear system of equations. However, interpolations with higher-degree polynomials through suboptimally spaced points are well-known to be prone to oscillations known as Runge's phenomenon. This effect arises because the interpolating polynomial needs to pass exactly through each interpolation point. Therefore, the polynomial must oscillate between the points, leading to increasingly large deviations, particularly near the ends of the interval.

To guarantee the minimal oscillatory solution, points at the Chebyshev nodes of the first kind, also known as Chebyshev zeros, were used for interpolation (Ref. 10). Nodes for a Chebyshev polynomial of degree n are given by the following relation:

$$x_n = \cos\left(\frac{2k+1}{2n}\pi\right), \quad k = 0, \ldots, n-1. \tag{8}$$

Using Chebyshev zeros for the interpolation also allows for the use of the discrete Chebyshev transform for calculating the polynomial coefficients,

$$a_n = \frac{p_n}{N} \sum_{m=0}^{N-1} u(x_m) T_n(x_m), \tag{9}$$

where N is the number of coordinates to be used for interpolation, u is the function to be approximated, and p_n is a function that is 1 when $n = 0$ and 2 otherwise. This transform allows for quick and efficient computation of the a_n coefficients without the need for solving a linear system of equations.

As described in the previous section, a general airfoil shape function may have an infinite slope at $x = 0$. To robustly eliminate this pathological behavior, a square root coordinate transformation, similar to the one used by Masters et al. (Ref. 11) is introduced,

$$\xi = \pm\sqrt{x}. \tag{10}$$

Masters et al. (Ref. 11) use the square root function as a spline parameterization centered at the leading edge to help increase smoothness at the leading edge. In this work, this transformation expands the unwanted singular slopes into ones that are finite. For instance, the form of the NACA thickness distribution can be rewritten as,

$$\eta\left(\xi\right) = a\xi + b\xi^2 + c\xi^4 + d\xi^6 + e\xi^8 \tag{11}$$

Granted, this coordinate transformation does not address functional behavior of $\eta\left(x\right)$ that can by expressed by x^N where $\frac{1}{2} < N < 1$.

Second, selecting the values of x according to the commonly used cosine distribution results in the values of ξ being coincident with the Chebyshev extrema points when uCST is employed. Therefore, using uCST with the proposed coordinate transform and a cosine distribution of points leads to the Chebyshev polynomials being a discretely orthogonal basis on ξ, which is a powerful property for representing the geometry.

The proposed transformation has been found to significantly improve the ability of uCST (and standard CST for that matter) to represent general airfoils. An illustrative example is included as Figure 2, which compares the ability of a 10^{th}-order Chebyshev approximation to represent the shape function of the NACA 2412. Without the transformation, the 10^{th}-order polynomial exhibits significant error and Runge phenomenon (induced by the infinite slope). With the proposed transformation, the 10^{th}-order approximation is remarkably improved.

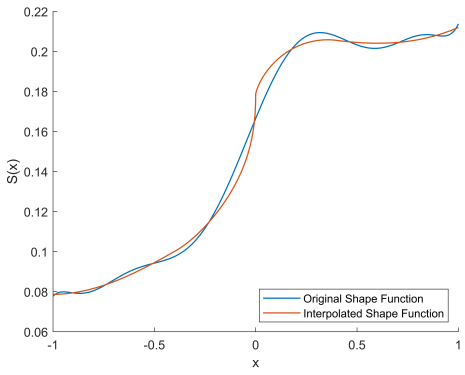

(a) Interpolation without coordinate transformation

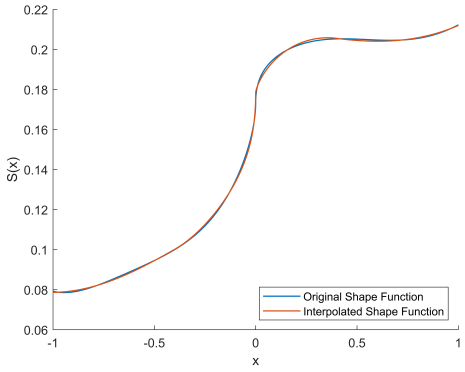

(b) Interpolation with coordinate transformation

Figure 2: Interpolation of the NACA 2412 airfoil shape function with and without a square root transform before interpolation.

AIRFOIL INTERPOLATION

Two ranges of NACA 4-digit series airfoils, from 1312 to 7720 and 0012 to 0020, were used as a test space for parameterization, because these ranges capture a wide range of thicknesses and cambers while remaining in the bounds of geometry that could be used on aircraft. Additionally, the NACA 4-digit series is defined by equations, meaning coordinates at specific values were able to be obtained without the need for interpolation. Airfoils were parameterized using different numbers of polynomial terms. These airfoils were then compared to the original airfoil by taking the norm of difference between the coordinates for each reconstructed airfoil. The mean of the norm was taken for all the airfoils and plotted with respect to the number of polynomial terms used for the reconstruction, shown in Figure 3. The figure shows that with more modes, the interpolated airfoils match the original airfoils more closely. This is to be expected, since the interpolation was done at the Chebyshev nodes, and as the number of polynomial modes approaches infinity, the interpolation becomes exact.

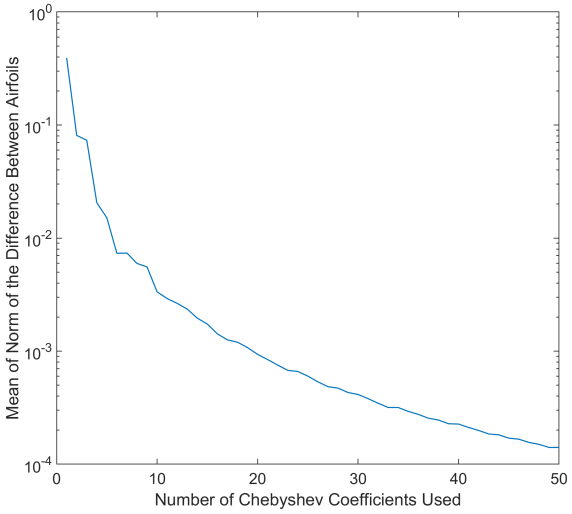

Figure 3: Average accuracy of the airfoil reconstruction plotted as a function of Chebyshev Modes.

To discern how many terms are needed to capture the aerodynamic characteristics of the airfoils, XFOIL simulations were conducted at a Reynolds number of 500,000 and a Mach number of 0.2, with parameterized airfoils using 10, 15, 20, 30, and 50 polynomial terms. XFOIL default values were used for all parameters not mentioned. Additionally, the airfoil was repaneled from 200 coordinate points to 200 panels using the pane command, also using the default values.

Tables 1, 2, and 3 contain the average differences between the of lift, drag, and pitching moment coefficients between the base airfoil and the reconstructed airfoils. These differences are shown for angles of attack of 0, 5, and 10 degrees, respectively. As the number of terms increases, the average difference between the coefficient values decreases. This is to be expected, because with more polynomial modes, the airfoil can be reconstructed more accurately. Overall, the results match well with the original airfoil with as little as fifteen polynomial modes.

Table 1: Average differences of coefficients at $\alpha = 0^\circ$.

# of Terms	Avg. Δcl	Avg. Δcd	Avg. Δcm
10	0.01195	0.00022	0.00248
15	0.00516	0.00014	0.00100
20	0.00340	0.00007	0.00069
30	0.00144	0.00003	0.00028
50	0.00042	0.00001	0.00008

Table 2: Average differences of coefficients at $\alpha = 5^\circ$.

# of Terms	Avg. Δcl	Avg. Δcd	Avg. Δcm
10	0.01205	0.00036	0.00229
15	0.00783	0.00024	0.00144
20	0.00319	0.00011	0.00063
30	0.00173	0.00003	0.00033
50	0.00044	0.00001	0.00008

Table 3: Average differences of coefficients at $\alpha = 10^\circ$.

# of Terms	Avg. ΔCl	Avg. ΔCd	Avg. ΔCm
10	0.01383	0.00054	0.00187
15	0.00733	0.00026	0.00104
20	0.00836	0.00029	0.00117
30	0.00281	0.00011	0.00039
50	0.00054	0.00002	0.00008

For a visual comparison, pressure distributions of the NACA 2414 at 10 and 15 degrees angle of attack are shown in Figures 4 and 5, respectively. It can be seen that, even with as little as 10 polynomial terms, the pressure distribution of the airfoil can be accurately captured with XFOIL. This may not be the case when performing analysis with higher-order methods that are more sensitive to small features in the geometry, such as oscillations introduced through the polynomial reconstruction.

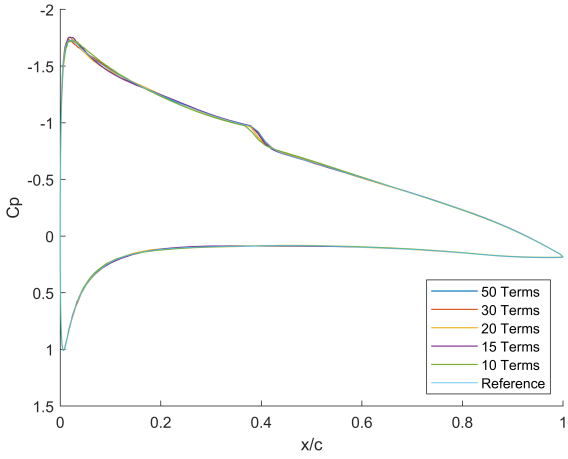

Figure 4: c_p distribution for NACA 2414 at $\alpha = 10^\circ$.

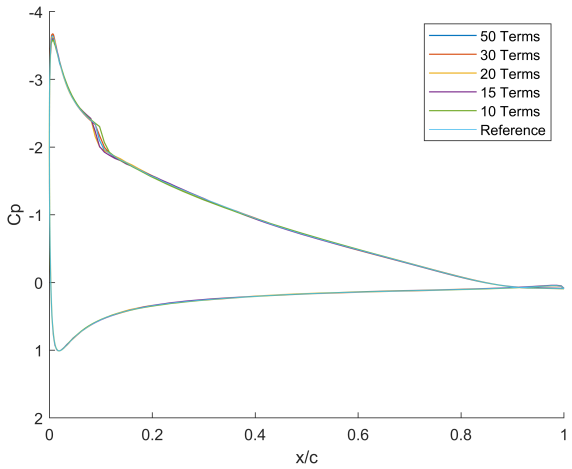

Figure 5: c_p distribution for NACA 2414 at $\alpha = 15^\circ$.

Non-Analytically Defined Airfoils

Airfoils not defined by analytical equations pose a particular challenge; in this paper, the VR-12 and RC-410 airfoils will serve as examples. Since these airfoils are described by discrete coordinates, the coordinate points need to be interpolated to obtain points located at the Chebyshev zeros. To maintain continuity at the leading edge, these coordinates were interpolated using spline interpolation as a function of the arc length. Since the coordinates at the precise Chebyshev nodes cannot be exactly obtained, a mock Chebyshev interpolation was used. This is where points that are close to Chebyshev nodes are chosen from a discrete set of data, which are then used for interpolation. Following the procedure for mock Chebyshev interpolation, a large number of points were generated along the spline and the points closest to the Chebyshev nodes were chosen for interpolation.

Before interpolation, an iterative method was used to place the leading edge of the airfoil, which was defined by spline interpolation, at the origin to within 1e−16. The leading edge in this paper was defined as the point furthest from the trailing edge because this guarantees that one x value corresponds to only one value on the upper surface and only one value on the lower surface. Otherwise, the shape function cannot be interpolated because it is not a one-to-one function. Furthermore, the class-shape transformation also requires a one-to-one function.

Despite these efforts, some shape functions are not ideal for interpolation. Figure 6 shows that there is a large jump discontinuity at the origin. On the other hand, some airfoils are much better behaved, the RC-410, shown in Figure 7, for example. However, there exists a hump to the left hand side of the origin. Even when this region is removed, the interpolation accuracy, shown in Figure 8, is more than an order of magnitude less converged than the average of the NACA 4-digit series used, shown in Figure 3.

Geometric convergence may not be the criterion for a parameterized airfoil when small oscillations are present, shown in Figure 9. These small oscillations may be significant when conducting simulations with higher-order methods, which then requires more modes to damp out. Therefore, the sensitivity of an analysis tool to these oscillations needs to be understood before using this method. Furthermore, it is seen in Figure 9 that the error is maximum near zero, stressing the importance of adequately managing the slope discontinuity at the origin.

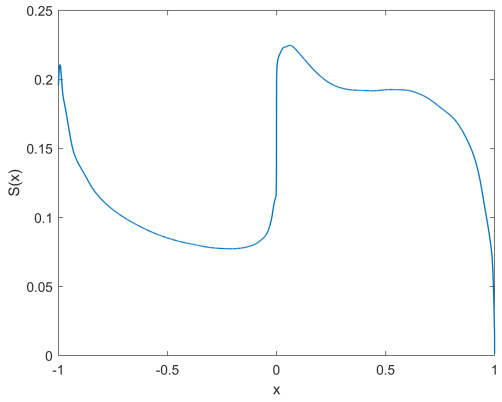

Figure 6: VR-12 airfoil in uCST space.

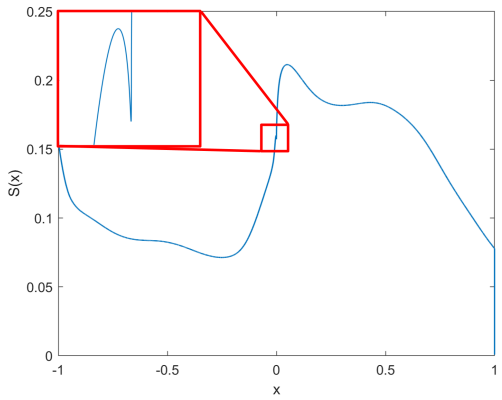

Figure 7: RC-410 airfoil in uCST space.

CLASS SHAPE TRANSFORMATION OBSERVATIONS

Unfavorable behaviors that occur when unwrapping non-analytically defined airfoils can be attributed to how CST addresses the leading-edge behavior of the airfoil, for which the $N1$ parameter is responsible. This parameter dictates the exponential behavior of the leading edge. A value of one-half assumes that the leading edge of the airfoil is circular, while values greater than one-half and less than one-half correspond to sharper and blunter leading edges, respectively. This is a key point in understanding why some airfoils do not cooperate with the unwrapped CST method for a general value of one-half for the $N1$ parameter.

Suppose that the leading-order term that describes the shape of the leading edge of the airfoil takes the form of ax^b, where b is the exponent and a is a coefficient that scales the function

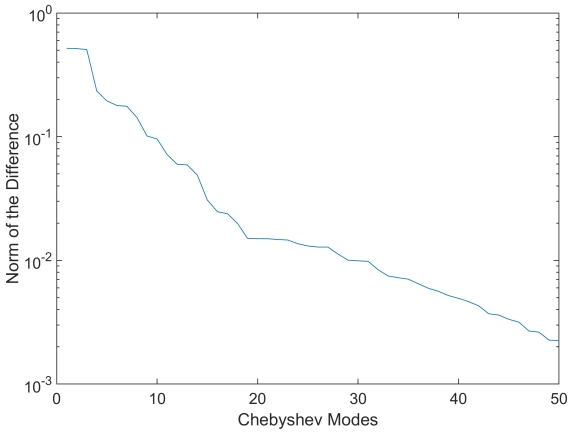

Figure 8: RC-410 approximation as a function of Chebyshev Modes.

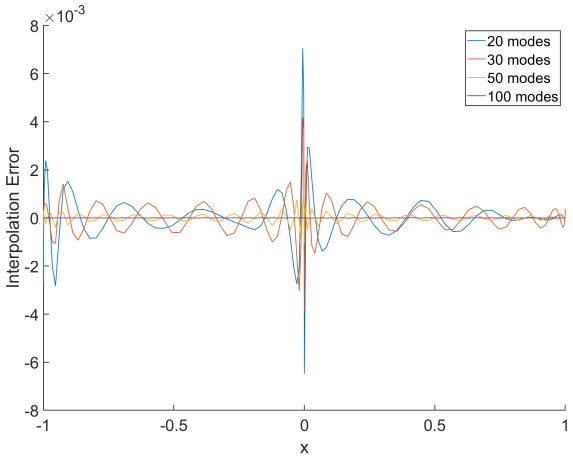

Figure 9: Difference between the exact and approximated shape functions of an RC-410.

in the y direction. When the CST is applied, the b exponent determines whether the function will converge. If b is exactly $N1$, the function will converge to the constant a. Alternatively, if $b > N1$, the shape function will approach zero at the origin. Conversely, when $b < N1$, the shape function will approach infinity at the origin when viewed in uCST space. However, airfoils without an analytical definition may have more complex leading-edge behaviors. The VR-12 airfoil, shown in Figure 6, converges to two different values at the origin. In contrast, a rapid change in curvature on the lower surface of the RC-410 causes a small hump to appear on the left side of the origin, shown in Figure 7. The CST requires the dominant leading-edge behavior to be of the form ax^b, however, this proves to be too reductive of a description for these cases.

The previous conclusions also explain why the uCST works exceptionally well for unwrapping the NACA 4-digit series airfoil family. The equations for the camber line and thickness distributions are defined by

$$z_c(x) = \begin{cases} \frac{m}{p^2}(2px - x^2), & 0 \le x < p \\ \frac{m}{(1-p)^2}\left((1-2p) + 2px - x^2\right), & p \le x \le 1 \end{cases} \quad (12)$$

and

$$z_t(x) = 5t(0.2969\sqrt{x} - 0.1260x - 0.3516x^2 + 0.2843x^3 - 0.1015x^4), \quad (13)$$

respectfully, where p is the location of maximum camber, m is the maximum camber, and t is the maximum thickness. Knowing that the square root term dominates near the origin, the rest of the terms may be ignored for the purposes of this analysis. Taking the limit shows that the shape function will always converge to a value of $1.4845t$ at the origin. It will always be continuous, but not necessarily smooth.

These peculiarities make the use of the uCST method for general airfoil parameterization unruly because careful characterization and treatment of the leading edge would be required by tuning the $N1$ parameter for a wide variety of airfoils. Even with this tuning, the shape function can still be difficult to interpolate, because the leading edge of the airfoil may have different behavior on the upper and lower surfaces.

OUTLOOK AND FUTURE WORK

The CST method is not the best method for unwrapping an airfoil where the leading-edge behavior does not comport with the assumptions made by the class function. Therefore, other, more general parameterizations should be explored. One with great potential that has been identified builds on the Theodorsen-Garrick method (Ref. 12) as implemented by Coder (Ref. 13). In this approach, the airfoil (with an assumed closed trailing edge) is subjected to an inverse Kármán-Trefftz transformation,

$$\left[\frac{\zeta - \zeta_1}{\zeta - \zeta_2}\right] = \left[\frac{z - z_1}{z - z_2}\right]^{\frac{1}{n}}, \quad (14)$$

where z is the complex coordinate in the airfoil plane, ζ is the complex coordinate of the transformed shape, and n is defined by the trailing-edge included angle. In the ζ plane, the airfoil maps to a pseudo-circle as shown in Fig. 10 (from (Ref. 13)).

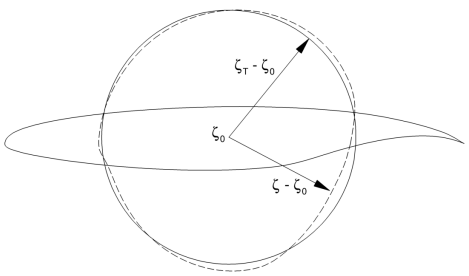

Figure 10: Mapping an airfoil to a pseudo-circle (from (Ref. 13)

The pseudo-circle, ζ, can be mapped to an exact circle, ζ_T, using a stable fixed-point iteration described in (Ref. 12). Once ζ_T is known, one can define, based on Eppler (Ref. 14),

$$P(\phi) + iQ(\phi) = \ln\left(\frac{dz}{d\zeta_T}\right) - \ln\left(1 - \frac{1}{\zeta_T}\right), \tag{15}$$

for which

$$P(\phi) = -\ln\left[\frac{V(\phi)}{2\left|\cos\left(\frac{\phi}{2} - \alpha\right)\right|}\right] \tag{16}$$

contains the velocity distribution and

$$Q(\phi) = \tan^{-1}\left(\frac{dy}{dx}\right) - \frac{\phi - \phi|_{\theta=0}}{2} \tag{17}$$

contains the geometry. These functions satisfy the Lighthill constraints (Ref. 15), which may be expressed as

$$\int_0^{2\pi} P(\phi)\, d\phi = 0 \tag{18}$$

$$\int_0^{2\pi} P(\phi)\cos(\phi)\, d\phi = \pi \tag{19}$$

$$\int_0^{2\pi} P(\phi)\sin(\phi)\, d\phi = 0. \tag{20}$$

Since $P(\phi)$ and $Q(\phi)$ are conjugate harmonic functions, similar integral relations can be defined for $Q(\phi)$ that are ultimately redundant. Every closed airfoil has a unique $P(\phi)$ and $Q(\phi)$ that is periodic on $\phi = [0, 2\pi]$ and satisfies the Lighthill constraints, and every periodic $P(\phi)$ and $Q(\phi)$ that satisfies the Lighthill constraints yields a closed airfoil.

A representative example of the $P(\phi)$ function is shown in Fig. 11. The behavior near $\phi = \pi$ is typical of leading edges and is present in all airfoils, and the steep slope near $\phi = \pi/2$ is from an intentional design feature of this airfoil.

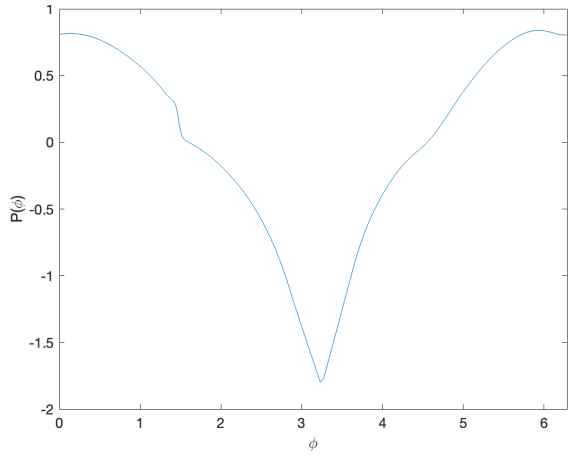

Figure 11: Representative $P(\phi)$ function for an airfoil.

CONCLUSION

An improved Chebyshev representation using a square root mapping for airfoil parameterization was introduced. The Class Shape Transformation (CST) was first used to unwrap NACA 4-digit series airfoils, which were then interpolated. Using a square root mapping, which expands the region around the origin, before interpolating greatly aided in reducing the Runge phenomenon. Interpolations showed that this method can accurately parameterize a range of NACA 4-digit airfoils using as few as ten Chebyshev polynomial modes, yielding a mean error norm of 0.003. Analysis of the reconstructed airfoils in XFOIL corroborated this conclusion. However, difficulties arise when trying to parameterize airfoils that are not defined by equations, because the leading-edge shape may not be exactly elliptic. An elliptic behavior of the leading edge is required for the parameters chosen for the CST method in this paper. As a result, the behavior of the shape function at the leading edge makes acquiring a parameterization difficult. Therefore, a more generalized unwrapping method, which builds upon the Theodorsen-Garrick method, is suggested. This method overcomes the lack of smoothness at the origin found with CST method, which will aid in attaining more accurate interpolations.

REFERENCES

1. Greenwood, E., Brentner, K. S., Rau, R. F., and Ted Gan, Z. F., "Challenges and Opportunities for Low Noise Electric Aircraft," *International Journal of Aeroacoustics,* Vol. 21, (5–7), 2022, pp. 315–381. DOI: 10.1177/1475472X221107377

2. Masters, D. A., Taylor, N. J., Rendall, T. C. S., Allen, C. B., and Poole, D. J., "Review of Aerofoil Parameterisation Methods for Aerodynamic Shape Optimisation," AIAA 2015-0761. 53rd AIAA Aerospace Sciences Meeting. Kissimmee, Florida, January 5–9 2015. DOI: 10.2514/6.2015-0761

3. Kulfan, B., "A Universal Parametric Geometry Representation Method -"CST"," AIAA 2007-62, 45th AIAA Aerospace Sciences Meeting and Exhibit, Reno, Nevada, January 8–11, 2007. DOI: 10.2514/1.29958

4. Drela, M., "XFOIL: An Analysis and Design System for Low Reynolds Number Airfoils," *Low Reynolds Number Aerodynamics. Lecture Notes in Engineering*, Vol. 54, 1989, pp. 1–12. DOI: 10.1007/978-3-642-84010-4_1.

5. Stanko, J., "Automated Design And Evaluation Of Airfoils For Rotorcraft Applications," Master's thesis, The Pennsylvania State University, 2017.

6. Anusonti-Inthra, P., "Airfoil Parameterization Using an Orthogonal Class Shape Transformation," AIAA 2024-2140. AIAA SCITECH 2024 Forum. Orlando, Florida, January 8–12 2024. DOI: 10.2514/6.2024-2140

7. Sridharan, A., and Sinsay, J. D., "Accelerating Aerodynamic Design of Rotors using a Multi-Fidelity Approach in TORC: Tool for Optimization of Rotorcraft Concepts," AIAA 2023-4305. AIAA AVIATION 2023 Forum. San Diego, California, June 12–16, 2023. DOI: 10.2514/6.2023-4305

8. Vassberg, J., Harrison, N., Roman, D., and Jameson, A., "A Systematic Study on the Impact of Dimensionality for a Two-Dimensional Aerodynamic Optimization Model Problem," AIAA 2011-3176. 29th AIAA Applied Aerodynamics Conference. Honolulu, Hawaii, June 27–30, 2011. DOI: 10.2514/6.2011-3176

9. Karman, M., McNamara, M., and Coder, J. G., "Airfoil Optimization via the Class-Shape Transformation and Orthogonal Deformation Modes," AIAA 2019-3173. AIAA Aviation 2019 Forum. Dallas, Texas, June 17–21 2019. DOI: 10.2514/6.2019-3173

10. Higham, N. J., Dennis, M. R., Glendinning, P., Martin, P. A., Santosa, F., and Tanner, J., *The Princeton Companion to Applied Mathematics*, Princeton University Press, Princeton, Part IV, Subpart 9, NJ, 2015, pp. 248–251.

11. Masters, D. A., Taylor, N. J., Rendall, T. C. S., Allen, C. B., and Poole, D. J., "Geometric Comparison of Aerofoil Shape Parameterization Methods," *AIAA Journal*, Vol. 55, (5), 2017, pp. 1575–1589. DOI: 10.2514/1.J054943

12. Theodorsen, T. and Garrick, I. E., "General Potential Theory of Arbitrary Wing Sections," NACA Report 452, 1934.

13. Coder, J. G., "Design of Low-Speed Slotted, Natural-Laminar-Flow Airfoil Reproducing Transonic Behaviors," *Journal of Aircraft*, Vol. 58, (3),2021, pp. 526–535. DOI: 10.2514/1.C035887.

14. Eppler, R., and Somers, D. M., "A Computer Program for the Design and Analysis of Low-Speed Airfoils," NASA-TM-80210, 1980.

15. Lighthill, M. J., "A New Method of Two-Dimensional Aerodynamic Design," Aeronautical Research Council, R&M 2112, England, UK, 1945.